A thermodynamic multiphase scheme treating polymer crystallization and melting

G. Strobl[a]

Physikalisches Institut, Albert-Ludwigs-Universität Freiburg, 79104 Freiburg, Germany

Abstract. A comparison of transition and melting temperatures of n-alkanes with experimentally determined ticknesses and melting points of polyethylene lamellae shows that the variation of the thickness with the crystallization temperature virtually agrees with the chain length dependence of the crystalline-mesomorphic phase transition in n-alkanes. Mesomorphic polyethylene layers are stable objects up to the thickness set by this phase transition. The findings lend further support to the view that polymer crystallization generally uses a route which includes a passage via a mesomorphic phase. We construct a thermodynamic scheme dealing with the transitions between melt, mesomorphic layers and lamellar crystallites, assuming for the latter ones that they exist both in an initial "native" and a final "stabilized" form. Application of the scheme in a reconsideration and quantitative evaluation of SAXS and DSC results previously obtained for PE, sPP, iPS and P(ϵCL) yields the equilibrium transition temperatures between the various phases, latent heats of transition and surface free energies. According to the results the mesomorphic phases are not liquid-like, but have thermodynamic properties which place them truly intermediate between melt and crystals.

PACS. 61.41.+e Polymers, elastomers, and plastics – 64.70.-p Specific phase transitions – 64.60.My Metastable phases

1 Introduction

Conventional wisdom assumes a growth of the lamellar polymer crystallites by direct attachment of chain sequences from the melt onto a lateral growth face. For many years there were no experimental observations which would have spoken against this natural view, and theories like the ones developed by Hoffman and Lauritzen [1] or by Sadler [2], which were formulated on this basis, were able to describe the temperature dependence of growth rates of many polymer systems quite well. Experiments and theories in fact directed the main focus on the growth rate, due to its technical importance and the many simple ways to measure it. These theories imply as a basic law that crystal thicknesses should be controlled by the supercooling below the equilibrium melting point T_{f}^{∞}, decreasing inversely with that supercooling – apart from a temperature invariant small excess which is required to provide a driving force. Surprisingly and hard to accept for many, a direct check of this relationship by time – and temperature dependent small angle X-ray scattering experiments did not confirm this law. Comprehensive investigations carried out for various crystallizable polymers led to the general result that crystal thicknesses are inversely proportional to the supercooling below another temperature,

called T_{c}^{∞}, which is always located many degrees above T_{f}^{∞}. An even more drastic deviation from classical predictions was found for statistical copolymers. While T_{f}^{∞} decreases, as expected, with a rising fraction of co-units, the crystal thickness remains invariant and equal to that of the homopolymer. On the other hand, when the thicknesses were measured at the melting points by SAXS experiments during heating, they fully confirmed the Gibbs-Thomson equation [3,4]. We thought – and are still convinced – that the conclusion which has to be drawn from these observations is unambiguous: crystallization and melting are not reverse processes – the pathway followed during the growth of polymer crystallites differs from that during melting. In fact, we were not the first ones coming up with such a view. In the beginning of the 1990ies, Keller and his co-workers Goldbeck-Wood, Hikosaka and Rastogi had already presented clear-cut evidence for such a case [5]. If crystallization experiments are carried out for polyethylene at an elevated pressure just below the triple point value, one observes a crystal formation via a transient mesomorphic "hexagonal" phase. The process can be directly followed using a polarizing optical microscope. Crystals nucleate into the hexagonal phase, then grow to sizes in the micrometer range, before they finally transform into the orthorhombic phase after a second, statistically initiated nucleation step. The melting upon

[a] e-mail: `gert.strobl@physik.uni-freiburg.de`

subsequent heating then takes place directly, without a passage through the hexagonal phase. Authors interpreted their observations as a new example for Ostwald's rule of stages [6]. This rule, formulated about 100 years earlier, states that crystals always nucleate into that mesomorphic or crystalline structure which is the most stable one for nm-sized crystals. Due to differences in the surface free energy this state may differ from the crystal modification which is macroscopically stable.

Thinking about our own results, which were all obtained at normal pressures, we felt that Ostwald's rule of stages might provide a clue to an understanding here as well. The observed different controlling temperature, T_c^∞ rather than T_f^∞, then would have to be related to a phase transition associated with a transient mesomorphic phase. Obviously, it was not possible to just take over the scheme proposed by Keller and his co-workers. Crystal thicknesses are sharply selected under normal pressure conditions, which differs from the statistically induced transformation process observed at elevated pressures. The model which we developed to describe the results therefore showed differences in the character of the steps and included additional features [7]. While the first step in crystal growth is again the attachment of chain sequences onto the growth face of a mesomorphic layer with minimum thickness, which is in the second stage again followed by a spontaneous thickening, we assume that a solidification of the mesomorphic layer takes place exactly at the point where a certain critical thickness is reached. The solidification produces crystallites which not only have a well-defined thickness but also a well-defined lateral extension, both with values in the nm-range. Such a granular substructure of the lamellae is suggested by measured line widths of wide angle X-ray scattering reflections and sometimes also directly by AFM and TEM images. Our model assumes that the "native" crystallites formed in the first place further stabilize in time, i.e., decrease their Gibbs free energy by a change of the surface structure.

We introduced this model in purely qualitative manner, in order to provide basic explanations for the observed dependencies. In particular, it accounted for the different relationships found between the crystallization temperature T_c and the crystal thickness d_c, addressed by us as "crystallization line" when plotted in the form $d_c^{-1}(T_c)$, and between the crystal thickness and the melting point as given by the "melting line" $d_c^{-1}(T_f)$ which agrees with the Gibbs-Thomson equation [8]. The model furthermore yielded a natural explanation for the invariance of the crystal thickness with regard to the co-unit content in statistical copolymers: if the co-units are already rejected when the mesomorphic phase forms they have indeed no influence on the final crystal thickness.

We now proceed a step further. There exist convincing arguments supporting the view that the crystallization line measured for polyethylene can indeed be identified with a thickness dependent phase transition between the hexagonal and the orthorhombic modification. They will be presented at first. We then introduce a thermodynamic multiphase scheme which can be generally used for a description and interpretation of observable structure changes taking place during the crystallization and melting of polymers. On the basis of this scheme our previous SAXS and DSC measurements can be reconsidered and now evaluated. This will be illustrated in a discussion of data obtained for polyethylene (PE), syndiotactic polypropylene (sPP), both for homopolymers and statistical copolymers, and furthermore, for poly(ϵ-caprolactone) (PϵCL) and isotactic polystyrene (iPS).

We begin with a brief summary of important properties of the hexagonal phase of polyethylene and its impact on crystallization.

2 Summary of properties of the mesomorphic phase in n-alkanes and polyethylene

For pressures above 3.2 kb a mesomorphic phase, known as "hexagonal phase", shows up in polyethylene as a stable phase, in addition to the orthorhombic-crystalline and the liquid phase. Figure 14 depicts in the upper part the phase diagram as it was obtained by Dollhopf and Leute using a high pressure dilatometer [9]. The phase diagram indicates that in this high pressure range a cooling from the melt leads at first into the stability range of the hexagonal phase before on further cooling the crystalline state is reached. If a sample is kept in the stability range of the hexagonal phase, at first thin layers form which then spontaneously thicken to macroscopic sizes. When the transition into the crystalline phase is induced by cooling after a prolonged thickening period one ends up in the nearly completely crystalline, "extended chain morphology" of polyethylene. The extended chain morphology thus represents the signature of a passage through the mesomorphic phase. Chains in the hexagonal phase possess an overall stretched conformation which incorporates, however, gauche-defects in form of kinks in a similar concentration as in the melt. Considering the internal energy and entropy of the hexagonal phase, it is closer to the liquid than to the orthorhombic-crystalline state; the latent heats Δh_{am} and Δh_{ac} of transitions from the melt into the mesomorphic and crystalline phase respectively have a ratio $\Delta h_{am}/\Delta h_{ac}$ of about 0.3.

An intermediate phase between the crystalline state and the melt is also found in n-alkanes, for chains with less than about 40 carbon atoms. Their range of existence during a heating process is of the order of some degrees. This phase is often addressed as "rotator phase", since a chain reorientation about the long axis constitutes the main aspect of disorder. Also here some kink defects exist, but only in low concentrations and preferentially near to the end-groups. This intermediate phase is more crystal- than liquid-like. The ratio between the heats of transition amounts to $\Delta h_{am}/\Delta h_{ac} \approx 0.7$.

There exist peculiar cases where a mesomorphic phase is also found for polyethylene at normal pressures. This occurs when the chains are chemically modified by irradiation, or if a mechanical field is applied on ultrahigh molar mass polyethylene fibers, so that the shrinkage which
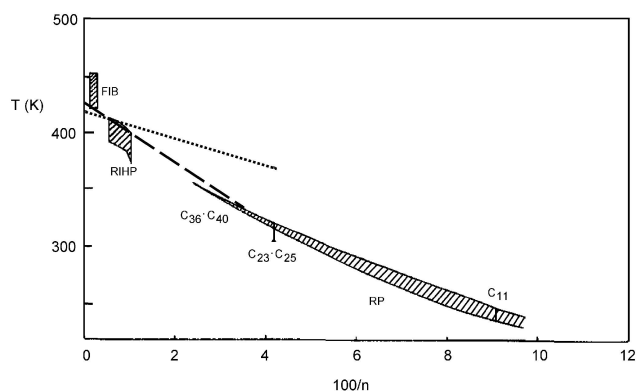
Fig. 1. From Ungar [10]: stability ranges of the mesomorphic phase at normal pressure, for various n-alkanes (rotator phase "RP"), irradiated polyethylene (radiation induced hexagonal phase "RIHP") and a length-fixed ultrahigh molar mass PE fiber ("FIB"); n is the number of carbons in the molecule or crystal stem. Crystallization line (*broken*) and melting line (*dotted*) of PE from Figure 5.

Fig. 2. PE for a pressure below the triple point value: temperature dependencies (schematic) of the bulk chemical potentials of the mesomorphic (hexagonal) and the crystalline (orthorhombic) phase. The potentials are referred to the chemical potential of the melt and denoted Δg_{am} and Δg_{ac} respectively.

usually accompanies the melting is at first suppressed. X-ray scattering patterns obtained for these two cases indicate the occurrence of a mesomorphic phase similar to the hexagonal high pressure phase, but now under normal conditions.

With these findings the question arises whether or not all these intermediate phases are related in the sense that their character changes continuously from the rotator phase of the n-alkanes to the hexagonal phase of a polyethylene at high pressures and temperatures. Ungar dealt with this question in a thorough analysis and arrived at the conclusion that, indeed, there exists one mesomorphic phase only [10]. It was in particular vibrational spectroscopy, carried out for the different systems, by which he demonstrated that there is a continuous change in the conformational statistics, when going from short chain n-alkanes to longer chain n-alkanes, then to irradiated and length-fixed polyethylene and, finally, taking into account the associated high temperature, to the hexagonal high pressure phase of polyethylene. Figure 1, taken from Ungar's work, depicts the results obtained for normal pressures. It shows the stability ranges of the mesomorphic phase as it is found for n-alkanes, irradiated polyethylene and a length-fixed ultrahigh molar mass polyethylene. The upper boundary always gives the transition line between the melt and the mesomorphic phase, and the lower boundary that between the mesomorphic phase and the crystalline state. It is obvious that there is a smooth continuation from the n-alkanes to the polyethylene states.

The figure indicates that for polyethylene special measures are required – chemical perturbations, mechanical forces or pressures – to have a stable mesomorphic phase. Without these measures it is metastable only, having thermodynamically a character as it is indicated in the drawing of Figure 2. The figure shows in a schematic plot for both the crystalline phase (c) and the mesomorphic phase
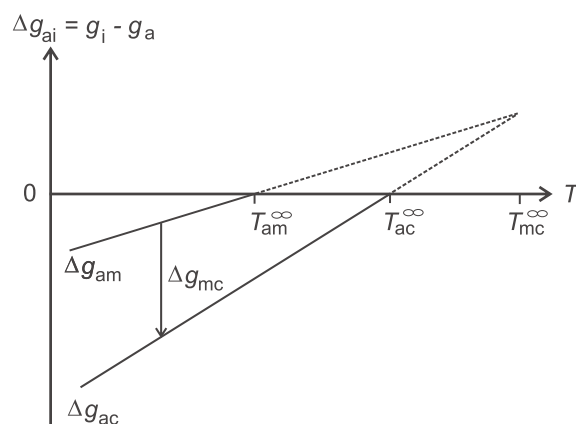
(m) the difference of the bulk chemical potential with regard to the melt (a):

$$\Delta g_{ac} = g_c - g_a,$$
$$\Delta g_{am} = g_m - g_a. \tag{1}$$

Coming from high temperatures the chemical potential of the crystalline phase drops below the value of the melt when crossing the equilibrium melting point T_{ac}^{∞}. The mesomorphic phase requires a lower temperature to fall with its chemical potential below that of the melt, here at T_{am}^{∞}. In the sketched case, which is representative for polyethylene under normal conditions, the chemical potential of the crystals is always below that of the mesomorphic phase. Hence, here the mesomorphic phase can be metastable only. The scheme includes also a temperature T_{mc}^{∞}. It represents the temperature of a virtual transition, namely that between the mesomorphic and the crystalline phase.

Thermodynamics relates the three transition temperatures T_{am}^{∞}, T_{ac}^{∞}, T_{mc}^{∞} to the heats of transition Δh_{ac} and Δh_{am}. Since the slopes of Δg_{am} and Δg_{ac} are given by the entropy changes Δs_{am} and Δs_{ac} respectively, one can write

$$(T_{mc}^{\infty} - T_{ac}^{\infty})\Delta s_{ac} = (T_{mc}^{\infty} - T_{am}^{\infty})\Delta s_{am}, \tag{2}$$

and therefore obtains

$$\frac{\Delta h_{am}}{\Delta h_{ac}} \approx \frac{\Delta s_{am}}{\Delta s_{ac}} = \frac{T_{mc}^{\infty} - T_{ac}^{\infty}}{T_{mc}^{\infty} - T_{am}^{\infty}}. \tag{3}$$

This equation can be used – and we shall apply it later on – if the heat of transition Δh_{am} is known. Data given by Dollhopf and Leute [9], obtained by high pressure calorimetry allow an estimate. Figure 3 suggests how an estimate can be obtained. While the heat of transition between the crystalline state and the melt can be determined for all pressures, corresponding data for the transition between the mesomorphic phase and the melt can only be
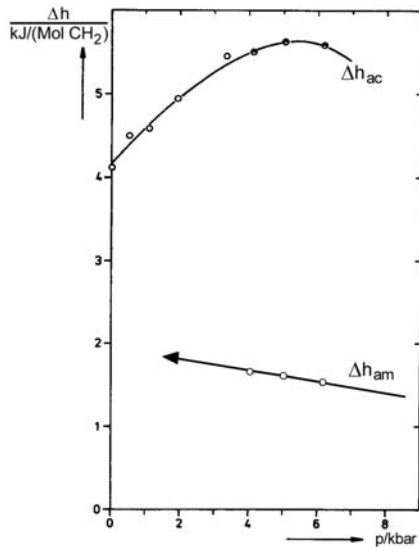
Fig. 3. PE: variation with pressure of the total heat of crystal melting Δh_{ac} and, above p_t, of the heat of transition Δh_{am}. From Dollhopf and Leute [9].

Fig. 4. From Keller and co-workers [6]: phase diagram (schematic) for lamellar PE crystallites of thickness n (structure units per stem) for a pressure below the triple point value: stability regions of the melt (a), of layers of the hexagonal phase (m) and of orthorhombic lamellar crystallites (c). Pathway followed in the crystallization processes observed in experiments carried out close to the triple point: nucleation into the hexagonal phase (1), successive growth through the m-region into the c-region, transformation into an orthorhombic crystal somewhere within the c-region initiated by a further nucleation step; the thickness at the crossing point X was in the μm-range.

obtained within the stability range of the mesomorphic phase, *i.e.*, for high pressures. For an estimate of Δh_{am} at normal pressures one can try to obtain data by carrying out a linear extrapolation. As indicated in the figure, this suggests choosing a value which is roughly half of Δh_{ac}.

3 Impact of the mesomorphic phase on the crystallization of polyethylene

Keller and his co-workers picked up Ostwald's concept of a size dependence of thermodynamic stabilities in the manner expressed by Figure 4. The figure shows a phase diagram in terms of temperature and size, whereby the inverse crystal thickness serves as size parameter. The thickness is given by the number n of structure units in a stem, *i.e.*,

$$n = \frac{d_c}{\Delta z} \qquad (4)$$

with d_c describing the layer thickness and Δz denoting the stem length increment per structure unit. The situation under consideration is that of Figure 2 where the crystal phase can get stable, but the mesomorphic phase remains metastable for all temperatures. Here, one has always $T_{mc}^{\infty} > T_{ac}^{\infty} > T_{am}^{\infty}$. The (T/n^{-1}) phase diagram in Figure 4 indicates that this sequence and thus stabilities can change for small enough crystallites. The prerequisite is a sufficiently low surface tension of the mesomorphic layer in the melt. The melting point depression with decreasing thickness then can be smaller than the one of the crystalline lamellae, with the consequence of an inversion of the transition temperatures. The inversion sets in at a crossing point X where the Gibbs free energies of equally thick crystalline and mesomorphic lamellae placed in the melt become identical. The phase diagram is composed of three stability regions associated with the amorphous
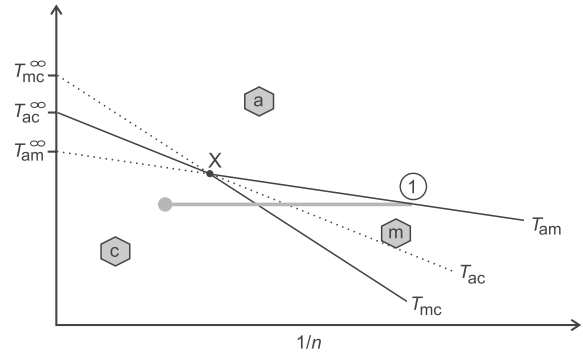
melt (a), layers of the hexagonal mesomorphic phase (m) and orthorhombic lamellar crystals (c). The phase boundaries, *i.e.*, transition lines are denoted T_{am}, T_{ac} and T_{mc}, all three representing functions of n^{-1}. The consequence of such given conditions for the formation and growth of crystallites is obvious: for temperatures below that associated with the crossing point, thin mesomorphic layers can become stable and thus form from the melt. The system uses this kinetically prefered pathway. The horizontal line starting at point 1 indicates the development. The first step is the formation and further growth of a mesomorphic layer with a minimum thickness as given by the transition line $T_{am}(n^{-1})$. The high inner mobility of the mesomorphic phase makes a spontaneous thickening possible which transfers the layer into the stability range of the crystal lamellae (c). Somewhere in this range the transition into the crystalline state then takes place, initiated by a nucleation step. This is exactly what was observed in the experiments. A simultaneous lateral and longitudinal growth could be seen directly in a polarizing optical microscope which stopped when after a statistically initiated nucleation the transformation into the crystalline state occurred. Hikosaka devised a nucleation theory which describes the whole process [11]. The process, found at high pressures just below the triple point, concerns mesomorphic and crystalline objects with thicknesses and lateral extensions in the μm-range.

Might an interference of the hexagonal phase also control the crystallization of polyethylene under normal pressure? Keller and co-workers who had already speculated about this saw some possibility, but could not provide a proof. We are now convinced that this indeed happens, and can prove it by experimental data. SAXS experiments were carried out for two polyethylenes with octene co-units and they led to the results shown in Figure 5 [4].

Table 1. Polyethylene and poly(ethylene-*co*-octene): thermodynamic data following from the experiments.

	T_{mc}^{∞}	T_{ac}^{∞}	T_{am}^{∞}	$T(X_{\mathrm{n}})$	$T(X_{\mathrm{s}})$	Δh_{ac}	Δh_{am}	$\sigma_{\mathrm{ac_n}}$	$\sigma_{\mathrm{ac_s}}$	σ_{am}
	°C	°C	°C	°C	°C	$\frac{\mathrm{kJ}}{\mathrm{mol\ C_2H_4}}$	$\frac{\mathrm{kJ}}{\mathrm{mol\ C_2H_4}}$	$\frac{\mathrm{kJ}}{\mathrm{mol}}$	$\frac{\mathrm{kJ}}{\mathrm{mol}}$	$\frac{\mathrm{kJ}}{\mathrm{mol}}$
P(EcO14)	154	133	112	100	99	8.2	4.1	7.5	6.6	1.2
PE	154	144	134	130	129	8.2	4.1	7.5	6.6	1.2
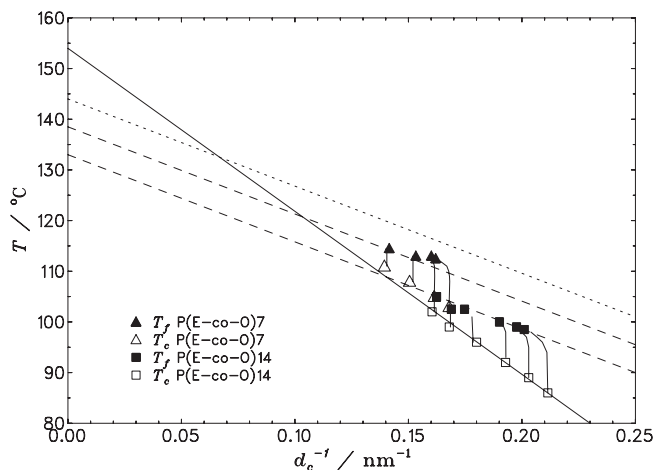
Fig. 5. P(EcOx): crystallization line T_{c} versus d_{c}^{-1} (*continuous, open symbols*) and melting lines T_{f} versus d_{c}^{-1} (*dashed, filled symbols*). The dotted line is the extrapolated melting line of polyethylene [4].

Shown (with open symbols) are the crystal thicknesses measured during and after isothermal crystallizations at various temperatures between 85 °C and 110 °C – there was no thickening during the crystallization time – and (with filled symbols) the melting points registered during subsequent heating runs. As expected one finds a difference in the Gibbs-Thomson melting lines for the two samples with 7 and 14% per weight of octene units, with lower values for P(EcO14), but, in contrast to that, a virtually unique dependence of the crystal thickness on the crystallization temperature, *i.e.*, only one crystallization line. The same result was obtained earlier for syndiotactic polypropylene and a series of related octene copolymers (see Fig. 8) and also in a recent additional SAXS study on a broader series of copolymerized polyethylenes [12]. On the basis of the two measured melting lines one can estimate the course of the melting line of pure polyethylene (we avoided direct measurements on non-copolymerized polyethylene, because here thickness values are always modified by the ongoing crystal thickening processes – a property of polyethylene and all other polymers with activated sliding motions within the crystals). It is also included in the figure, ending at 144 °C close to the equilibrium melting point of polyethylene as given by Flory and Vrij [13] based on a thermodynamic analysis of *n*-alkane melting points ($T_{\mathrm{f}}^{\infty} = 145$ °C). When we plot the crystallization line and the (extrapolated) melting line of polyethylene into Ungar's phase diagram Figure 1, noteworthy results show up. The first one concerns the melting

points: comparing crystalline layers with the same thickness n it can be stated that the *n*-alkanes melt at much lower temperatures than polyethylene. The reason follows from the analysis carried out by Flory and Vrij. Polyethylene crystals with a thickness n melt when

$$ng_{\mathrm{c}} + 2\sigma_{\mathrm{ac}} = ng_{\mathrm{a}} \qquad (5)$$

where σ_{ac} denotes the excess surface free energy per crystalline stem end. For *n*-alkanes the Gibbs free energy per molecule in the melt is further reduced, due to the delocalization of the CH_3-endgroups. This delocalization – or "unpairing" of the endgroups, using Flory's words – can be accounted for by formulating the equilibrium condition at the melting point of *n*-alkanes as

$$ng_{\mathrm{c}} + 2\sigma_{\mathrm{ac}} = ng_{\mathrm{a}} - RT \ln n. \qquad (6)$$

The $RT \ln n$-term relates to the translational entropy of the molecules. While the translational entropy is completely negligible for polymers, it always has to be included in treatments of smaller molecules; for low molar masses it becomes even dominant. When Flory and Vrij evaluated the *n*-alkane melting point data they derived in addition to the equilibrium melting point also the following value of $2\sigma_{\mathrm{ac}}$:

$$2\sigma_{\mathrm{ac}} = (2200 + 2.2 \times 418) \text{ cal mol}^{-1} = 13 \text{ kJ mol}^{-1}$$

using

$$\Delta h_{\mathrm{ac}} = 950 \frac{\mathrm{cal}}{\mathrm{mol\ CH_2}} = 8.0 \frac{\mathrm{kJ}}{\mathrm{mol\ C_2H_4}}.$$

When we derive $2\sigma_{\mathrm{ac}}$ from the slope of the PE melting line we obtain for the surface free energy (see Tab. 1)

$$2\sigma_{\mathrm{ac}} = 13.1 \text{ kJ mol}^{-1} \qquad (7)$$

i.e., somewhat unexpected considering the different surface structures, an almost identical value. Hence, the close approach of the hexagonal-melt to the orthorhombic-hexagonal transition in the *n*-alkane phase diagram is due to the translational entropy contribution only. Since the latter is absent in the melting process of polyethylene, the stability range for mesomorphic polyethylene layers with thicknesses in the nm-range – comparable to the *n*-alkanes – becomes much expanded. These layers thus represent under normal pressure conditions indeed stable objects.

The second noteworthy finding concerns the crystallization line. As can be seen, it nearly coincides with and *linearly continues the at first slightly bent line* associated
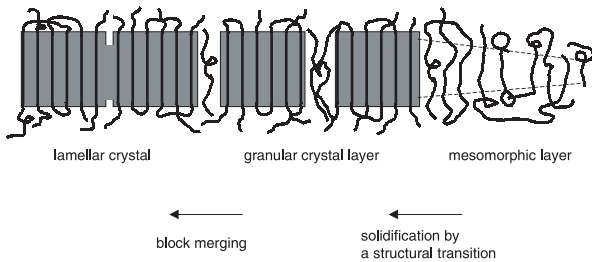
Fig. 6. Sketch of the pathway followed in the growth of polymer crystallites as suggested in reference [7].

Fig. 7. (T/n^{-1})-phase diagram for polymer layers in a melt ("a") dealing with 3 phases: mesomorphic "m", native crystalline "c_n" and stabilized crystalline "c_s". Two pathways for an isothermal crystallization followed by heating, A (low crystallization temperatures) and B (high crystallization temperatures): (1) chain attachment onto a mesomorphic layer with a thickness determined by the transition line T_{am}; (1)–(2) spontaneous layer thickening; (2) formation of native crystals when the thickness reaches the transition line T_{mc_n}. The then following stabilization of the crystallites causes a change of the related transition lines and a shift of the crossing point from X_n to X_s. Pathway A during heating: upon reaching the transition line T_{mc_s} (3a) onset of continuous recrystallization processes up to the melting at X_s (3b). Pathway B during heating: the crystallites melt when T_{ac_s} is reached (3). The experimental "crystallization line" is identical with T_{mc_n}, the "melting line" is identical with T_{ac_s}, the "recrystallization line" is to be identified with T_{mc_s}.

with the mesomorphic-crystalline phase transition of the n-alkanes. Since the endgroup location in the interfaces of the n-alkane crystal is retained at this transition, no translational entropy arises and there is no difference between polyethylene and n-alkane layers. The observed coincidence therefore tells us something, namely, that the crystal thickness d_c is obviously selected exactly by this transition. The selection is sharp; there is no evidence for any excess thickness as it is required to stimulate the nucleated transition in the high pressure experiments of Keller and co-workers. The cause of the difference in the transformation properties – both are first order transitions – could be related with the size: here, we are in the nm-range, the transition concerns nm-blocks for which it could be an easy collective process, whereas the high pressure experiments refer to the μm-range where the transition requires an activated nucleation.

4 Thermodynamic scheme describing polymer crystallization and melting

In our first attempt to interpret the different dependencies observed for the crystallization and melting process we proposed the model reproduced in Figure 6 [7]. It is meant to describe different stages which are passed through when a lamellar crystallite is growing. Taking up Keller's idea the process starts with an attachment of chain sequences from the melt onto a growth face of a mesomorphic layer with minimum thickness which then spontaneously thickens. When a critical thickness is reached, the layer solidifies immediately under the formation of block-like crystallites. The existence of blocks was suggested both by wide-angle X-ray scattering experiments which indicate that the coherence length in lateral direction has the same order of magnitude as the crystal thickness, and also by direct observations in the AFM, which often show such a blocky structure [14,15]. Even more, according to recent observations crystal thickness and lateral coherence length are strictly correlated [16]. Their ratio is temperature invariant, suggesting that the crystal block formation out of a transient mesomorphic phase is an elementary step in polymer crystallization. A last, but equally important step in the crystal development is a stabilization of the crystallites in time, leading to a further decay in the Gibbs' free energy. It can be formally described as a decrease in the surface free energy. In the model of Figure 6 this last
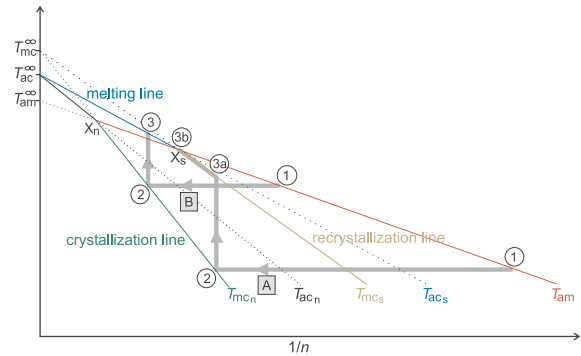
step is addressed as a "merging" of the blocks, but this represents only one possibility.

When we proposed this model the question about the nature of the transient mesomorphic phase was left open. One view under consideration was a near-to-liquid state like a nematic liquid crystal – the existence of such a precursor phase had been proposed by Kaji and co-workers [17] or Winter and co-workers [18] on the basis of experiments, or by Olmstedt [19] on a theoretical basis. An alternative was a truly intermediate state similar or equal to that found in the high pressure experiments of the Keller group. We now think that we are able to decide this issue. Not only the presented comparison between polyethylene and n-alkane data, but also the result of evaluations which follow strongly support to identify, in the case of polyethylene, the mesomorphic phase with the known hexagonal phase, and to assume also for the other crystallizing polymer systems the existence of a mesomorphic phase with similar intermediate character.

We address the stabilization as a process which transforms the initial "native" crystals into "stabilized" crystals and thus deal with the following phases:

- the amorphous melt, marked by the label "a";
- mesomorphic layers (label "m");
- native crystals (labelled "c_n") and
- stabilized crystals (with label "c_s").

In the spirit of Ostwald's rule of stages we set up for these phases the scheme displayed in Figure 7. It is devised to

treat the process of a crystal development under isothermal conditions and to follow the structural changes during a subsequent heating – just as experiments are usually carried out. The thermodynamic conditions to which the scheme refers are the same as for Figure 4, namely bulk transition temperatures in a sequence $T_{mc}^\infty > T_{ac}^\infty > T_{am}^\infty$ as it is found at normal pressures. However, dealing with two different crystalline states, native crystals and stabilized crystals, two different crossing points are encountered. They are denoted X_n and X_s. Their positions control what happens during an isothermal crystallization followed by heating. There are two different scenarios, exemplified by the pathways A and B in the figure. In experiments these are realized by crystallizations at low or high temperatures respectively, usually emanating from the glassy state in the former case, or coming directly from the melt in the latter. We first address the high temperature case, i.e., pathway B. At the point of entry, labelled "1", chains are attached from the melt onto the lateral growth face of a mesomorphic layer with the minimum thickness. The latter is determined by the melt-mesomorphic transition line T_{am}. The layer spontaneously thickens until the transition line T_{mc_n} is reached at point "2", where native crystals form immediately. The subsequently following stabilization transforms them into a lower surface free energy state (still at "2"). The consequence of the stabilization shows up during a subsequent heating. Without stabilization a heating would immediately transform the native crystals back into the mesomorphic state, but after the stabilization the situation has changed: since the crossing point is shifted to location X_s, the crystallites remain stable upon heating until the next transition line is reached. As shown by the scheme, this transition is now a direct melting without the interference of a mesomorphic phase. Exactly this is observed in many experiments in the case of a crystallization from the melt.

The structural changes to be expected along the pathway A are different. The beginning is the same – starting at point 1 with an attachment of chain sequences onto a spontaneously thickening mesomorphic layer, then, on reaching T_{mc_n}, the formation of native crystals followed by a stabilization. Heating the stabilized crystals they at first retain their structure. However, as shown in the scheme, at first the transition line T_{mc_s} is reached which relates to a transformation into the mesomorphic state instead of a crystal melting. The consequences are obvious ((3a) to (3b)): a repetition follows of the same two steps again and again, first a transition into the mesomorphic phase and then a thickening until crystals form. The end of this multi-sequence is reached at the crossing point X_s where the crystal melts. Experimental examples to be given further on show exactly these structural changes.

Thermodynamics fixes the different transition lines denoted $T_{mc_n}, T_{ac_n}, T_{mc_s}, T_{ac_s}, T_{am}$, all to be understood as functions of n^{-1}. T_{ac_s} relates to the equilibrium between stabilized crystals and the melt where

$$g_c + \frac{2\sigma_{ac_s}}{n} = g_a. \tag{8}$$

σ_{ac_s} describes the surface free energy per crystal stem end for a stabilized layer in the melt. With

$$g_a - g_c \approx \frac{\Delta h_{ac}}{T_{ac}^\infty}(T_{ac}^\infty - T) \tag{9}$$

we obtain

$$T_{ac}^\infty - T \approx \frac{2\sigma_{ac_s}T_{ac}^\infty}{\Delta h_{ac}}\frac{1}{n}. \tag{10}$$

In experiments this line is addressed as the "melting line".

The experimentally obtained "crystallization line" is to be identified with the transition line T_{mc_n} giving the location of the equilibrium between mesomorphic and native crystalline layers of equal thickness, being established for

$$g_c + \frac{2\sigma_{ac_n}}{n} = g_m + \frac{2\sigma_{am}}{n}. \tag{11}$$

σ_{am} and σ_{ac_n} denote the respective surface free energies, again expressed per crystal stem end. With

$$g_m - g_c \approx \frac{\Delta h_{mc}}{T_{mc}^\infty}(T_{mc}^\infty - T) \tag{12}$$

we obtain for the crystallization line the equation

$$T_{mc}^\infty - T \approx \frac{(2\sigma_{ac_n} - 2\sigma_{am})T_{mc}^\infty}{\Delta h_{mc}}\frac{1}{n}. \tag{13}$$

As we shall see, experiments on cold crystallized samples yield the transition line T_{mc_s} which we address as "recrystallization line". It follows from equation (13) exchanging the surface tension σ_{ac_n} by σ_{ac_s}, which is the equivalent parameter associated with stabilized crystals:

$$T_{mc}^\infty - T \approx \frac{(2\sigma_{ac_s} - 2\sigma_{am})T_{mc}^\infty}{\Delta h_{mc}}\frac{1}{n}. \tag{14}$$

Of importance is also the transition between the melt and the amorphous state, described by the line T_{am}. As it relates to the equilibrium

$$g_m + \frac{2\sigma_{am}}{n} = g_a, \tag{15}$$

we can write, with

$$g_a - g_m \approx \frac{\Delta h_{am}}{T_{am}^\infty}(T_{am}^\infty - T), \tag{16}$$

$$T_{am}^\infty - T \approx \frac{2\sigma_{am}T_{am}^\infty}{\Delta h_{am}}\frac{1}{n}. \tag{17}$$

$T_{am}(n^{-1})$ begins at T_{am}^∞ and then passes through the two crossing points X_n and X_s. A knowledge of two of these three points is required in order to fix the a⇔m transition line.

On the basis of the thus established thermodynamic scheme we are now able to discuss our experimental results. We have studied the effect of co-units and diluents on crystallization and melting in polyethylene and s-polypropylene, and we will begin with a reconsideration of these experiments. Then the scheme will be applied
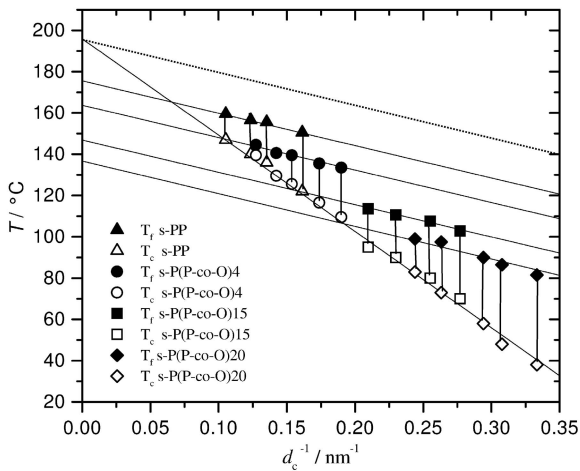
Fig. 8. sPP and sP(PcOx): unique crystallization line (*open symbols*) and series of melting lines (*filled symbols*); the dotted line is the extrapolated melting line of a perfectly syndiotactic polypropylene [20].

on a selection of existing published data. We shall deal with experiments carried out on polyethylene and copolymers, syndiotactic polypropylene and copolymers, isotactic polystyrene and poly(ϵ-caprolactone). Application of the scheme provides us with an understanding of the observations and enables a quantitative data evaluation to be carried out.

5 Effects of co-units and diluents

Of special importance for the start of a renewed discussion about the mechanism of polymer crystallization was the observed invariance of crystal thicknesses in series of copolymers with different co-unit contents. The first observations of this kind were made on syndiotactic polypropylene and related octene copolymers [3,20]. Figure 8 reproduces these data. While a whole series of melting lines appears, showing a melting point suppression which systematically increases with the octene co-unit content, there exists only a unique crystallization line, *i.e.*, a unique dependence of the crystal thickness on the crystallization temperature.

Parts of analogous findings for polyethylene and related copolymers have been presented in Figure 5. For one of the copolymer systems in this figure, P(EcO14), we studied additionally the effect of two different diluents, namely of the *n*-alkane $C_{16}H_{34}$ and of methylanthracene ($C_{15}H_{12}$) [21]. The results, reproduced in Figure 9, show that the effect of diluents can be different: a dissolution of methylanthracene again leaves the crystallization line unchanged, producing only a shift in the melting line, but the dissolution of *n*-$C_{16}H_{24}$ results in shifts of both the melting- as well as the crystallization line. The thermodynamic scheme provides an understanding, and the two different situations are dealt with in Figure 10. Effects depend on whether or not the diluent molecules or the
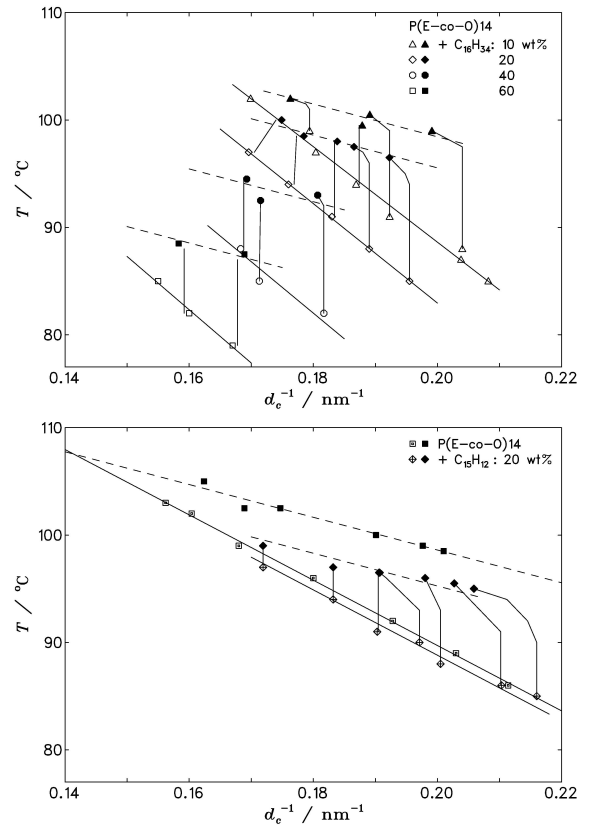

Fig. 9. Polymer-diluent mixtures P(EcO14)/$C_{16}H_{34}$ (90/10; 80/20; 60/40; 40/60): crystallization lines and melting lines (*top*). Mixtures P(EcO14)/$C_{15}H_{12}$ (100/0; 80/20): crystallization lines and melting lines (*bottom*) [21].

co-units can enter the mesomorphic phase. If they are rejected those transformation lines which include the melt, *i.e.*, T_{ac_n}, T_{ac_s} and T_{am}, are shifted to lower temperatures, but the line T_{mc} remains unaffected. This is the situation sketched in part b: the crystallization line does not change while the melting line experiences a shift, and this is observed for all co-units and for methylanthracene as a diluent. Another situation is encountered if the diluent becomes incorporated into the mesomorphic phase, and is only rejected subsequently when the crystals form. Under these conditions (part c) all transitions which include the crystalline state are shifted while the transition between the melt and the mesomorphic phase, T_{am}, remains on its place (the latter holds in the ideal case of a complete inclusion; if there is a partial rejection also T_{am} will shift). Such a situation is met if *n*-$C_{16}H_{24}$ is used as a diluent for polyethylene, which leads to a shifting of both the crystallization line T_{mc_n} and the melting line T_{ac_s}.

The amounts of shifting induced by a diluent can be derived from Raoult's law, in the case of the melting line as

$$T_{ac_s}^{\infty}(x_d = 0) - T_{ac_s}^{\infty}(x_d) = \frac{R(T_{ac_s}^{\infty})^2}{\Delta h_{ac}} x_d. \qquad (18)$$

Here, x_d denotes the molar fractions of dissolved molecules. The shifts in Figure 9 agree with equation (18) in satisfactory manner [21].
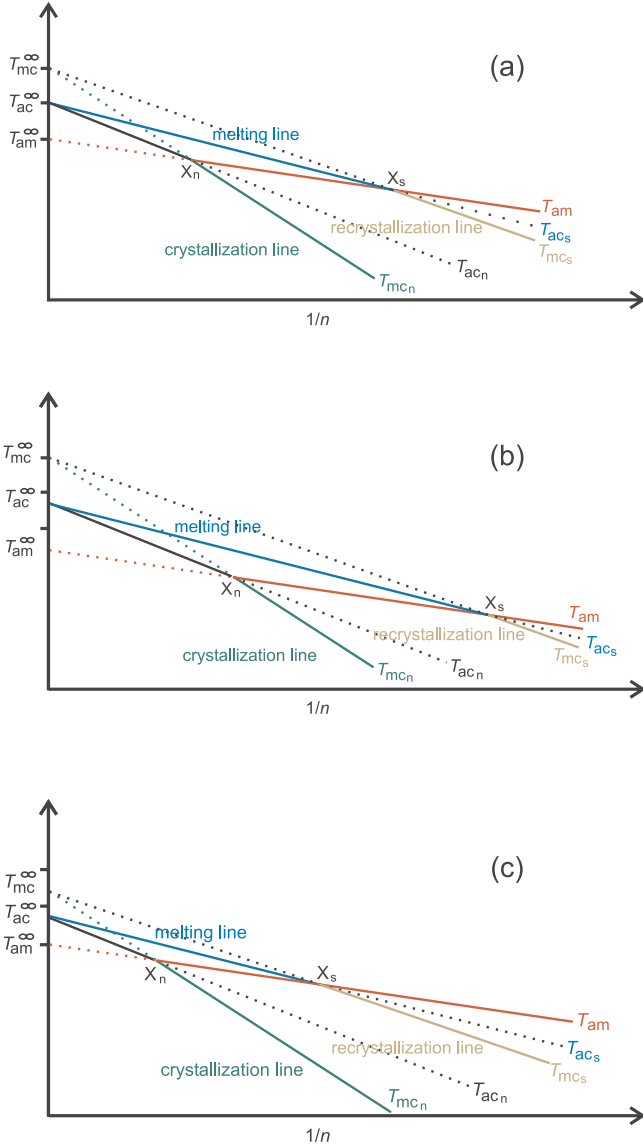
Fig. 11. Multiphase scheme applied to SAXS data of P(EcO14) [4]: crystallization line (*green*), melting line (*blue*), recrystallization line (*ocher*), crossing points X_s and X_n, $T_{am}^{\infty} = 112$ °C from equation (3) and a⇔m transition line (*red*).

Fig. 10. Variations in the (T/n^{-1})-phase diagram introduced by co-units and diluents: (a) homopolymer crystallization (b) effect of co-units or a diluent which remains in the melt: shift of the melting line but invariant crystallization line; (c) effect of a diluent which enters the mesomorphic phase: shifts of both the melting line and the crystallization line.

Flory suggested to use Raoult's law also for statistical copolymers [22], however, the experimental results, *i.e.*, the melting line shifts observed for the octene-copolymer of polyethylene shown in Figure 5 contradict this view. The shifts introduced by co-units are much larger than those of equal molar fractions of diluent molecules [21].

6 Application to various crystallizing polymer systems

6.1 Polyethylene and related copolymers

We first discuss data which were obtained for a polyethylene copolymerized with 14% per weight of octene co-units
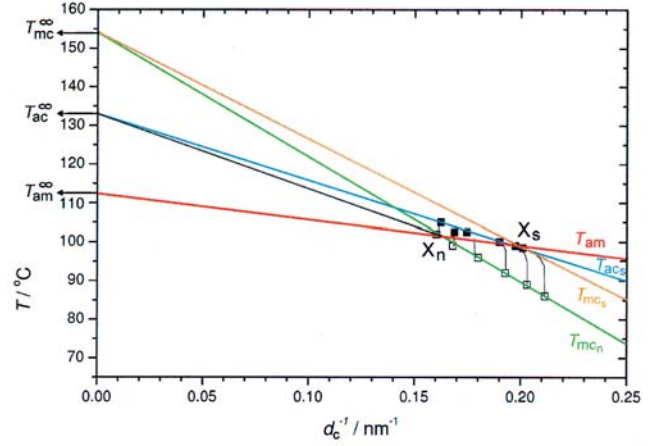
(P(EcO14)). The SAXS data obtained for this sample are included in Figure 5 and we extract them and depict them again in Figure 11. The crystallization line and the melting line are well defined by the data, and we draw them in green and blue color respectively. A look on measured DSC curves is also of interest, and data are reproduced in Figure 12. Crystallization temperatures were chosen between 77 °C and 94 °C, and one observes a pronounced change in the melting properties: there is a constant final melting point located at 100 °C as long as the crystallization temperature is below 91 °C; for higher crystallization temperatures the melting peak location moves together with the crystallization temperature. An analogous behaviour shows up in the SAXS determined melting points. Exactly such a behavior is predicted by the thermodynamic scheme. We therefore identify the constant melting temperature of 100 °C with the location of the crossing point X_s and draw the recrystallization line (ocher-colored) through this point. It remains the question how we could possibly fix the a⇔m transition line. It has to pass through X_s, but a second point is still needed. For this purpose we use T_{am}^{∞} which can be determined by applying equation (3). As mentioned earlier, we derive from Figure 3 for the ratio between the heats of transition the approximate value $\Delta h_{am}/\Delta h_{ac} \approx 0.5$, which gives $T_{am}^{\infty} \approx 112$ °C. The a⇔m transition line connecting T_{am}^{∞} and X_s is drawn in red color. The point of intersection between T_{am} and the crystallization line, T_{mc_n}, is the first crossing point X_n. With this we have fully established the scheme and can derive all thermodynamic parameters. They are collected in Table 1. The surface free energies σ_{ac_s} and σ_{am} followed from the slopes of the melting line and of the a⇔m transition line respectively, by applying equations (10) and (17). The surface tension associated with the native crystals, σ_{ac_n}, is to be derived from the slope of the line which connects T_{ac}^{∞} and X_n. We note that the stabilization process leads to a decrease of the surface free energy by about 14%. As to be expected,
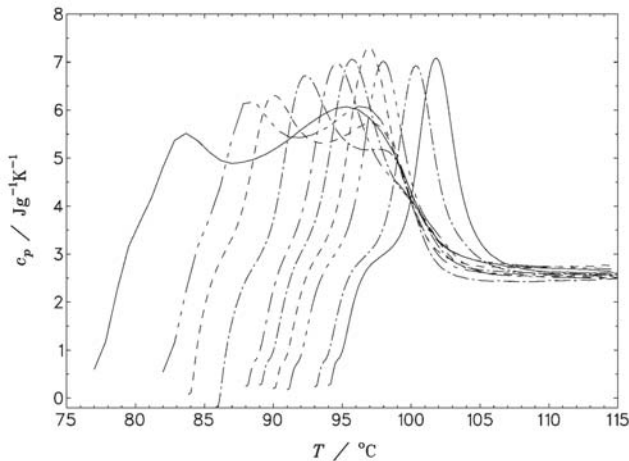
Fig. 12. P(EcO14): DSC curves measured subsequent to isothermal crystallizations at various temperatures between 77 °C and 94 °C, indicating a crossing point temperature $T(X_s) = 100$ °C.

the surface free energy of the mesomorphic layers is much smaller than that of the crystallites.

It is possible to establish the multiphase scheme also for polyethylene, and this is shown in Figure 13. The (green) crystallization line in the figure was directly transferred from Figure 5, the (blue) melting line is identical with the dotted line obtained by the extrapolation. In order to obtain T_{am}^∞ for polyethylene we again use equation (3) and obtain now an approximate value of 134 °C. The presence of co-units in the melt leads to a parallel shift of T_{am} to lower temperatures, however, the slope remains unchanged. We therefore can choose for the a⇔m transition line the same slope as in Figure 11. The now completed scheme includes also the two crossing points X_n and X_s. The data thus obtained for polyethylene are given in the second line of Table 1. Variations between P(EcO14) and PE are found only for the temperatures, not for the heats of transition and the surface free energies. To give an example for a possible crystallization and melting process following path B, a crystallization temperature of 127 °C is chosen (gray lines in Fig. 13). The pathway indicates that under these conditions at first a mesomorphic layer with an initial thickness of 8.9 nm would form. It would spontaneously thicken and change into the crystalline state at a thickness of 11.7 nm. The melting on heating would then occur at 131 °C. An actual experiment carried out for these conditions would, however, lead to slightly different results because polyethylene lamellae thicken also in the crystalline state, much less rapid than in the mesomorphic phase, but still measurable.

Having obtained values for the transition temperatures $T_{mc}^\infty, T_{ac}^\infty$ and T_{am}^∞, at least approximate ones, we can now speculate about a possible continuation of the m⇔c and a⇔m transition lines from the high pressure region, where they can be directly determined, down to normal pressure conditions. Figure 14 with the (p,T)-phase diagram
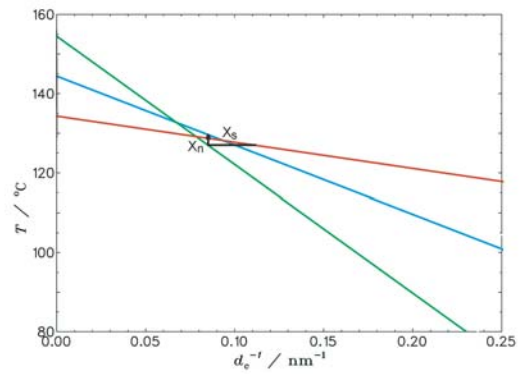

Fig. 13. Multiphase scheme applied to PE: crystallization line (*green*) and melting line (*blue*) from Figure 5, $T_{am}^\infty = 134$ °C from equation (3), slope of the a⇔m transition line $T_{am}(d_c^{-1})$ (*red*) from Figure 11. Pathway for a crystallization at 127 °C followed by a heating to the melt.

of polyethylene of Leute and Dollhopf [9] shows how this continuation could possibly look like.

6.2 s-polypropylene and related copolymers

We select here out of the series of samples in Figure 8 the sPP-copolymer with the highest octene content, sP(PcO20), and also a commercial sample with higher syndiotacticity, sPP-Mitsui, which was used in another investigation [23].

The SAXS data obtained for the commercial sample are shown in Figure 15. The sample was both, cold crystallized from the glassy state at 25 °C and crystallized from the melt at temperatures between 100 °C and 120 °C. The thicknesses for the various crystallization processes are all located on the (green) crystallization line. The changes of the thickness with temperature observed during heating greatly differ. For the three highest temperatures thicknesses remain constant up to the melting points. For the cold crystallized sample changes set in immediately when the heating starts. d_c^{-1} approaches and then follows the (ocher-colored) recrystallization line, until melting occurs near to or at the crossing point X_s. When crystallizations are carried out at 100 °C and 105 °C one meets the intermediate case: thicknesses remain constant until the recrystallization line is reached; from thereon d_c^{-1} follows this line. As is obvious, with a crystallization at the three highest temperatures one enters pathway B of the scheme, for the lower temperatures the structure changes during heating are those of pathway A.

The temperature at the crossing point X_s shows up also in the DSC scans, as can be seen in Figure 16. After an extended range of continuous reorganization, which extends up to 110 °C, crystals melt at about 130 °C independent of the heating rate, in agreement with the location of X_s found in the SAXS experiments. The (blue) melting line has to pass through the measured melting points. Its slope is already known from all the measurements carried out on sPP samples (see Fig. 8).
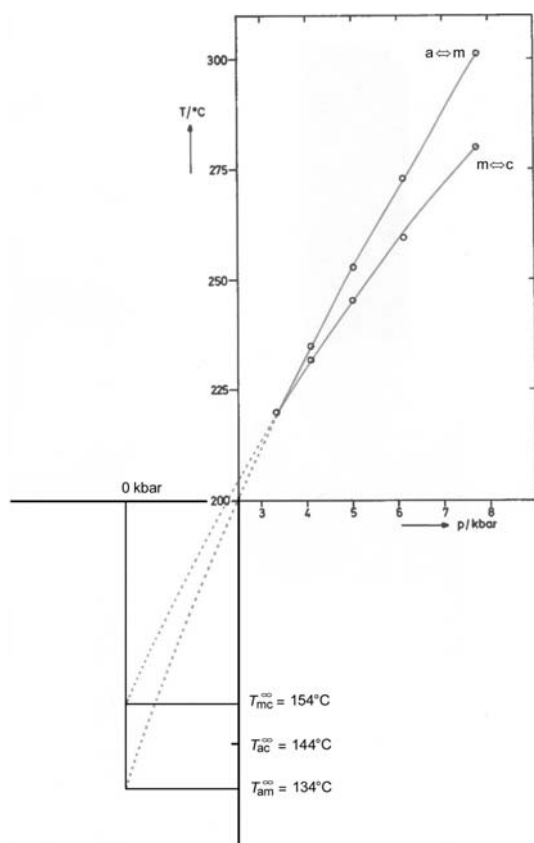
Fig. 14. pT-phase diagram of PE: stable mesomorphic phase above the triple point ($p_t \approx 3.3\text{kb}, T_t \approx 220\,^\circ\text{C}$, from Leute and Dollhopf [9]). A guess about the continuation of the (then virtual) transition lines a⇔m and m⇔c to normal pressure based on the experimentally determined crystallization and melting lines of PE.

Figure 17 collects the SAXS data which were obtained for sP(PcO20). The data for crystallization temperatures below 100 °C are extracted from Figure 8. Furthermore included are the results of three longtime measurements conducted at the highest temperatures [24,7]. A non-zero crystallinity was achieved here with the aid of the self-seeding technique. These experiments had been carried out in order to enter the temperature range where crystallization necessarily must produce thicknesses away from the crystallization line. This necessarily occurs for temperatures above $T(X_n)$. Usual crystallization experiments do not enter this range, because growth rates here become forbiddingly low; we also tried the experiment only in this single case. The data well fix the (green) crystallization and the (blue) melting line, and the line plotted through the three high temperature points – it represents T_{ac_n} – determines X_n. An additional DSC scan carried out for a cold-crystallized sample yielded the temperature location of X_s which turned out to be 80 °C. The now known locations of the two crossing points X_n and X_s allow to draw the (red) a⇔m transition line. With this, the scheme is fully established. In addition, since the slope of the a⇔m transition line does not vary between sPPs with different syndiotacticity or different co-units contents we use
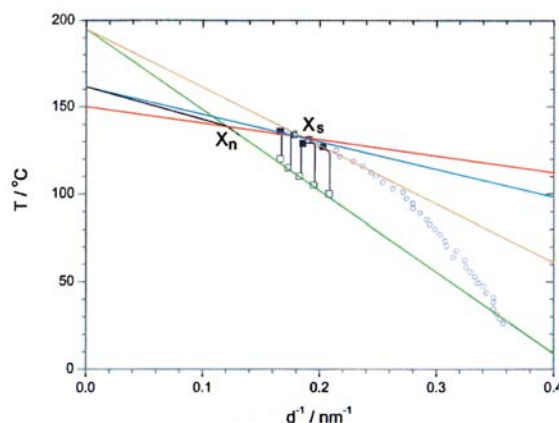

Fig. 15. SAXS data of sPP-Mitsui. (*Circles*) crystallization from the glassy state at 25 °C: variation of the crystal thickness during heating [23]. (*Squares*) melt crystallization at various temperatures between 110 °C and 120 °C followed by heating. Crystallization line (*green*), melting line (*blue*), recrystallization line (*ocher*), a⇔m transition line with slope from Figure 17 (*red*), crossing points X_n and X_s.
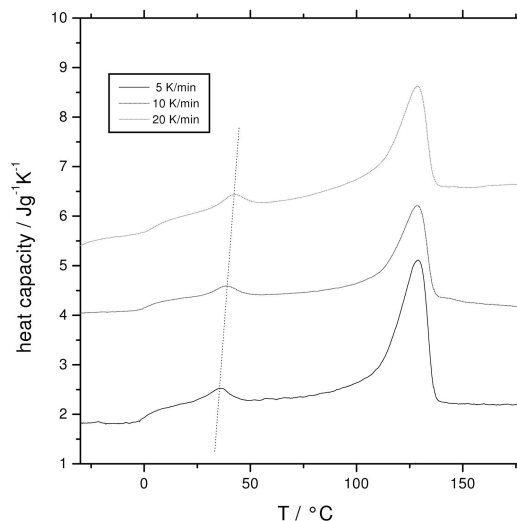

Fig. 16. sPP-Mitsui, quenched to the glassy state and then crystallized at 25 °C: DSC curves measured with the given heating rates, indicating a crossing point temperature $T(X_s) = 132\,^\circ\text{C}$. The low temperature endotherm shifts to lower temperatures when the heating rate is decreased.

this knowledge and plot also the a⇔m transition line into Figure 15. It has to pass through the crossing point X_s and now determines also the second crossing point, X_n.

Having adjusted the full scheme for both samples, all relevant thermodynamic data can be derived, and they are collected in Table 2. The heat of fusion $\Delta h_{\text{ac}} = 7.7$ kJ/mol C_3H_6 was taken from the literature. The heat of transition $\Delta h_{\text{am}} = 5.8$ kJ/mol C_3H_6 follows from equation (3), and the three surface free energies are derived from the slopes of the respective transition lines using the equations given previously.
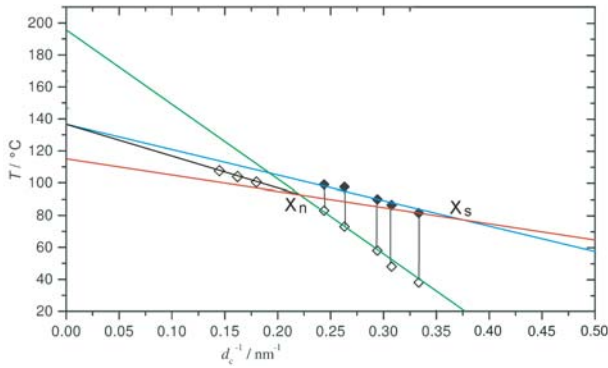
Fig. 17. SAXS data of sP(PcO20) [7]: Crystallization line (*green*), melting line (*blue*), crossing points X_n and X_s, a⇔m transition line (*red*).
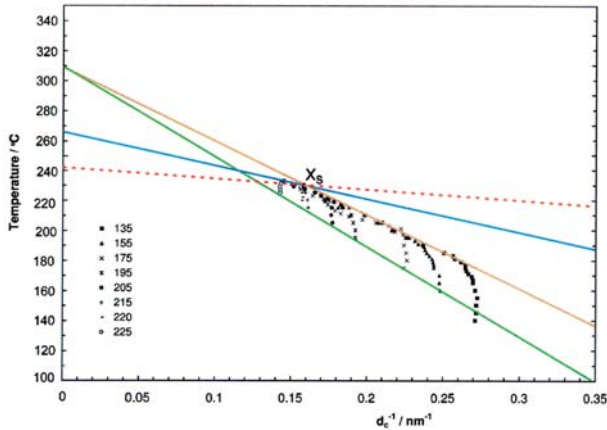

Fig. 18. SAXS data of iPS, showing the variation of d_c^{-1} during heating scans subsequent to isothermal crystallizations at the indicated temperatures [25]: crystallization line (*green*), melting line (*blue*), recrystallization line (*ocher*) and crossing point X_s. A possible course of the a⇔m transition line (*broken red*).

There is one further interesting, noteworthy point. Figure 8 includes also the melting line of a perfectly syndiotactic polypropylene as obtained by an extrapolation of all the measured melting lines. Different from the case of polyethylene, it appears as if the equilibrium melting point T_{ac}^{∞} of this ideal sample would coincide with T_{mc}^{∞}. This is exactly the situation at the triple point, where, even more, these two temperatures also coincide with T_{am}^{∞}, leading to

$$T_{mc}^{\infty} = T_{ac}^{\infty} = T_{am}^{\infty} = 195 \ ^\circ\text{C}.$$

Materials which are perfectly syndiotactic have not been synthesized so far. Obviously they would have interesting properties, for example, indeed follow pathway A – pathway B no longer exists – up to close to the equilibrium melting point. Furthermore, it can be expected that already some slight pressure would produce a macroscopically stable mesophase.
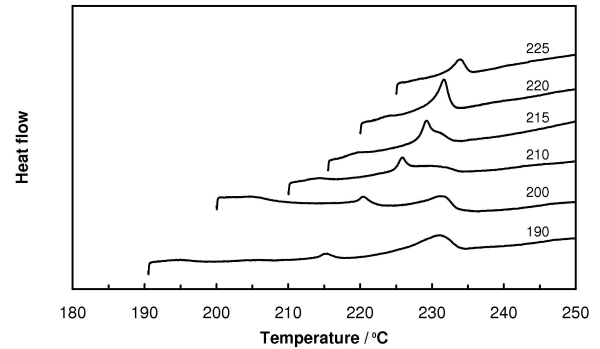

Fig. 19. iPS: DSC melting curves obtained after crystallizations at the given temperatures (heating rate 0.5 K/min), indicating a crossing point temperature $T(X_s) \approx 230 \ ^\circ\text{C}$ [25].

6.3 i-Polystyrene and poly(ϵ-caprolactone)

Finally, we reconsider in the framework of the new scheme SAXS and DSC data obtained earlier for a sample of isotactic polystyrene [25] and for poly(ϵ-caprolactone) [4].

Figure 18 reproduces SAXS data of the iPS sample. Crystallization experiments were carried out isothermally after a transfer from the amorphous glassy state. We measured the crystal thickness for various crystallization temperatures and then continued the measurement during heating processes up to the melting point. Again, two different scenarios are found. For low crystallization temperatures thicknesses remain constant at first, then increase, approach the recrystallization line, and finally follow this line up to the temperature of the crossing point X_s. On the other hand, for the highest crystallization temperatures no crystal thickening occurs up to the melting point. Data yield a well-defined crystallization line (plotted green) and also a well-defined recrystallization line (ocher). The melting line (blue) is less reliably determined due to the only small temperature interval within which melting points could be measured. The a⇔m transition line is not fixed by the data. It is only known that it has to pass through X_s with a negative slope, and the dotted red line included in the figure represents just a possible choice for illustration.

Figure 19 presents the corresponding DSC scans. In agreement with the SAXS observations the melting points reached in heating scans subsequent to isothermal crystallizations at lower temperatures are constantly located at about 230 $^\circ$C. This exactly agrees with $T(X_s)$. An upward move of the melting point together with an increasing crystallization temperature is found only at the highest temperatures, above 220 $^\circ$C.

One may ask about the meaning of the weak low temperature endotherm which varies with the crystallization temperature. As a check shows, its location is exactly on the recrystallization line. Hence, as it appears, these low temperature endotherms have to be associated with the transition from the crystalline to the mesomorphic phase. Since the recrystallization sets in immediately, the signal intensity is only low.

Table 2. s-Polypropylene and s-poly(propylene-*co*-octene): thermodynamic data following from the experiments.

	T_{mc}^{∞}	T_{ac}^{∞}	T_{am}^{∞}	$T(X_n)$	$T(X_s)$	Δh_{ac}	Δh_{am}	σ_{ac_n}	σ_{ac_s}	σ_{am}
	°C	°C	°C	°C	°C	$\frac{kJ}{mol\ C_3H_6}$	$\frac{kJ}{mol\ C_3H_6}$	$\frac{kJ}{mol}$	$\frac{kJ}{mol}$	$\frac{kJ}{mol}$
sPP-Mitsui	195	162	150	139	132	7.7	5.8	9.0	7.5	3.4
sP(PcO20)	195	137	113	92	80	7.7	5.8	9.0	7.5	3.4

Table 3. i-Polystyrene: some thermodynamic data derived from the experiments.

T_{mc}^{∞}	T_{ac}^{∞}	T_{am}^{∞}	$T(X_s)$	Δh_{ac}	Δh_{am}	σ_{ac_s}
°C	°C	°C	°C	$\frac{kJ}{mol\ C_8H_8}$	$\frac{kJ}{mol\ C_8H_8}$	$\frac{kJ}{mol}$
310	266	>230	230	9.3	>5.1	8.7

Table 4. Poly(ϵ-caprolactone): some thermodynamic data derived from the experiments.

T_{mc}^{∞}	T_{ac}^{∞}	T_{am}^{∞}	$T(X_s)$	Δh_{ac}	Δh_{am}	σ_{ac_s}
°C	°C	°C	°C	$\frac{kJ}{mol\ C_6H_{10}O_2}$	$\frac{kJ}{mol\ C_6H_{10}O_2}$	$\frac{kJ}{mol}$
135	100	>60	60	17.9	>8	8.4

Even if the thermodynamic scheme is not completely fixed by the data, one can still carry out an evaluation. The results are given in Table 3. The heat of fusion Δh_{ac} has been taken from the literature. From the slope of the melting line the surface free energy σ_{ac_s} can be derived. Not only the bulk transition temperatures T_{mc}^{∞} and T_{ac}^{∞} are determined by the data but also the crossing point temperature $T(X_s)$, following from both, the SAXS experiment and the DSC scans. $T(X_s)$ sets a lower limit for the unknown transition temperature T_{am}^{∞}. Applying equation (3) also gives a lower limit for Δh_{am}. It indicates that the mesomorphic phase is again in its properties intermediate between the melt and the crystalline phase.

Figures 20 and 21 present SAXS and DSC data obtained for poly(ϵ-caprolactone). The situation is similar to that encountered for i-polystyrene: depending on the chosen crystallization temperature one observes in the SAXS experiments both scenarios, structural changes during the heating for low temperatures, and an invariant thickness up to the melting point for high temperatures; the observations in the DSC scans correspond to that. Data again fix the crystallization line, the melting line and the recrystallization line and allow a determination of X_s. For illustration we also included in the figure a possible course for the a⇔m transition line (dotted red). The thermodynamic data derived from the experiments – again only a partial set – are collected in Table 4. Also for PϵCL we find for the mesomorphic phase properties which place it intermediate between the melt and the crystalline state rather than close to the liquid or the solid state.

7 Concluding remarks

As it appears, the consistency of the data representation within the framework corroborates the validity of the
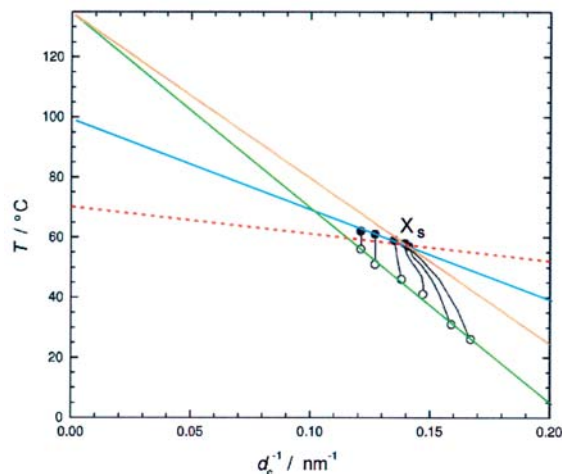
Fig. 20. SAXS data of PϵCL [4]: crystallization line (*green*), melting line (*blue*), recrystallization line (*ocher*) and crossing point X_s. A possible course of the a⇔m transition line (*broken red*).
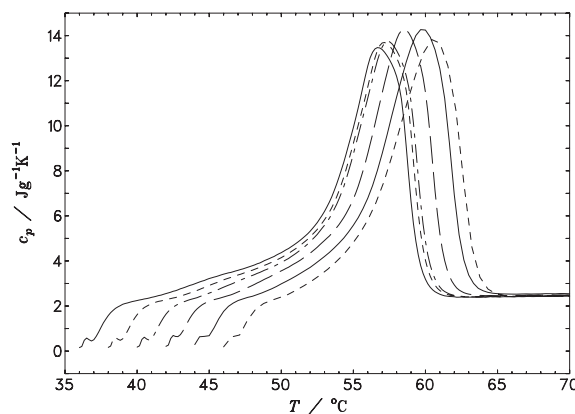
Fig. 21. PϵCL: DSC melting curves obtained after crystallizations at various temperatures between 37 °C and 47 °C (heating rate 10 K/min), indicating a crossing point temperature $T(X_s) = 60$ °C [4].

proposed thermodynamic multiphase scheme. In particular, the correct description of the two modes of structural changes upon heating after crystallizations at low and high temperatures looks very convinving. It may be surprising that a mesomorphic phase with properties right in the middle between the crystal and the melt should exist for all polymer systems, but the experiments indicate it quite clearly. Indeed, it is the interference of this mesomorphic phase which generally controls polymer crystallization via

the selection of the crystal thickness. Of equal importance for the non-reciprocity of crystallization and melting in polymer systems is the stabilization process which transfers the initial native crystallites into their final stabilized form.

Although not being particularly simple with its multitude of transition lines the proposed scheme still refers to an ideal case in the sense that it addresses the melting behavior of stabilized crystals only. As is demonstrated by the finding of straight Gibbs-Thomson melting lines, these possess definite properties, i.e., constant values of the heat of fusion and the surface free energy. In fact, as is known from various observations, not all the crystals experience a stabilization. In particular those which develop at later times often remain in the native or in an only partially stabilized state. Their presence shows up, for example, in the thickness change during heating of the cold-crystallized sPP shown in Figure 15. Stabilized crystals would not change their thickness up to the temperature at which the recrystallization line is reached, as it is observed for a crystallization at 100 °C. In case of the sample crystallized at room temperature thickness changes set in immediately, which indicates that at least a part of the lamellar crystallites has remained in the initial native state. Even a small temperature increase then brings them back into the mesomorphic state, from where they recrystallize again after some thickening. At the present state of investigation, there is not enough information on the nature of the stabilization process to incorporate it explicitly into the scheme.

Conventionally the stability variations showing up in the broad melting range observed also after an isothermal crystallization at high temperatures were primarily associated with thickness variations. However, this view is contradicted by the experiments. There was never an indication in the SAXS experiments for a change in the thickness distribution during heating. Our treatment therefore associates the variations in the crystal stability after an isothermal crystallization with variations in the surface free energy only.

Choosing straight lines for all the transitions in the phase diagram is of course an approximation, the same one which leads to the corresponding equations in Section 4. There are cases, where the data justify this linearization approximation, as for example the s-PP crystallization line in Figure 8 which straightly extends over a range of 100 °C. Existing curvatures would modify the three bulk transition temperatures, but it is difficult to estimate the amount of these changes and thus the accuracy of the values given in the tables.

Acknowledging the importance of the mesomorphic phase for the crystal formation in polymers a legitimate question comes up: why has its occurrence not been reported so far, or only in special cases like the polyethylene crystallization at high pressure? In particular, there exist now many AFM observations with high resolution but so far no images which would have the character of the sketch of Figure 8. The answer could be that the mesomorphic phase is passed through very rapidly, maybe even in the manner that it exists as a transient state during the formation of a block only. The block formation would then resemble the formation of a nucleus, and the building of a crystal lamella consequently a repeated self-supported and guided nucleation. That crystal nucleation can be facilitated by a passage through an intermediate phase is known since Ostwald's time, and it is corroborated by convincing experiments, for example, by the nucleation studies on n-alkanes carried out by Sirota et al. [26]. There could, however, also be another reason for the non-visibility of the mesomorphic phase in the AFM studies: its surface stiffness could be near to that of the crystal so that the contrast would be insufficient to show up in the images. Li et al. [27] reported in one work a certain weakness of the front zone of growing polyester lamellae and related it to perturbations of the crystal structure.

On the other hand, there exist signals for the transition into the mesomorphic phase which have already been observed by many people, namely, the often reported low temperature endotherms showing up in DSC scans a few degrees above the crystallization temperature. In the framework of the scheme not only the weak endotherms in the DSC scans of i-polystyrene in Figure 19, but also the low temperature endotherms in the curves observed for sPP-Mitsui (Fig. 16) have to be associated with a short transition of native crystals back into the mesomorphic state – short because it is immediately followed by a recrystallization. Typically, these signals move to lower temperature when the heating rate is decreased, as it is to be expected for a competition between a crystal dissociation and an immediate reformation.

If the mesomorphic phase extends only over a few nanometers and is passed through very rapidly one may ask about the justification of the use of the basically macroscopic notion of a "phase". In fact, such a use does not look problematic in view of the succesfull application of the Gibbs-Thomson equation for the melting point depression even for nm-sized crystals. Also important to note: assuming a passage through a transient mesomorphic phase differs from assuming the existence of a transition zone between crystal and melt with a continuous change of the state of order. A transition zone can always be incorporated into a thermodynamic treatment via an effective surface free energy. Then crystal sizes would be controlled by the supercooling below the equilibrium melting point, but this disagrees with the observations.

There exist certainly more questions and additional observations. Hopefully, the proposed scheme can serve as a sound basis to discuss them. It appears that it takes up main properties of polymer crystallization and melting in correct manner.

References

1. J.D. Hoffman, G.T. Davis, J.I. Lauritzen, Treatise on Solid State Chemistry **3**, edited by N.B. Hannay (Plenum 1976), p. 497
2. D.M. Sadler, G.H. Gilmer, Phys. Rev. B **38**, 5684 (1988)
3. G. Hauser, J. Schmidtke, G. Strobl, Macromolecules **31**, 6250 (1998)
4. B. Heck, T. Hugel, M. Iijima, E. Sadiku, G. Strobl, New J. Phys. **1**, 17 (1999)
5. S. Rastogi, M. Hikosaka, H. Kawabata, A. Keller, Macromolecules **24**, 6384 (1991)
6. A. Keller, M. Hikosaka, S. Rastogi, A. Toda, P.J. Barham, G. Goldbeck-Wood. J. Mater. Sci. **29**, 2579 (1994)
7. G. Strobl, Eur. Phys. J. E **3**, 165 (2000)
8. G. Strobl, *The Physics of Polymers* (Springer, 1997), p. 166
9. U. Leute, W. Dollhopf, Coll. Polym. Sci. **258**, 353 (1980)
10. G. Ungar, Macromolecules **19**, 1323 (1986)
11. M. Hikosaka, Polymer **31**, 458 (1990)
12. T.Y. Cho, B. Heck, G. Strobl, Coll. Polym. Sci. **282**, 825 (2004)
13. P.J. Flory, A. Vrij, J. Am. Chem. Soc. **85**, 3548 (1963)
14. T. Hugel, G. Strobl, R. Thomann, Acta Polym. **50**, 214 (1999)
15. S. Magonov, Y. Godovsky, Am. Lab. **31**, (1999)
16. T. Hippler, S. Jiang, G. Strobl, Macromolecules, in press (2005)
17. G. Matsuba, K. Kaji, K. Nishida, T. Kanaya, M. Imai, Polymer J. **31**, 722 (1999)
18. N.V. Pogodina, S.K. Siddiquee, J.W. van Egmond, H.H. Winter, Macromolecules **32**, 1167 (1999)
19. P.D. Olmsted, W.C.K. Poon, T.C.B. McLeish, T.C.B. Terrill, A.J. Ryan, Phys. Rev. Lett. **81**, 373 (1998)
20. B. Heck, T. Hugel, M. Iijima, G. Strobl, Polymer **41**, 8839 (2000)
21. B. Heck, G. Strobl, M. Grasruck, Eur. Phys. J. E **11**, 117 (2003)
22. P.J. Flory, Principles of Polymer Chemistry (Cornell University Press, 1953), p. 570
23. M. Grasruck, G. Strobl, Macromolecules **36**, 86 (2003)
24. T. Hugel, Diplomarbeit, Fakultät für Physik, Universität Freiburg (1999)
25. M. Al-Hussein, G. Strobl, Macromolecules **35**, 1672 (2002)
26. E.B. Sirota, A.B. Herhold, Science **283**, 529 (1999)
27. L. Li, C.M. Chan, K.L. Yeung, J.X. Li, K.M. Ng, Y. Lei, Macromolecules **35**, 316 (2001)